QUANTUM WELL INFRARED PHOTODETECTOR (QWIP) FOCAL PLANES FOR LONG WAVE INFRARED IMAGING

S. D. Gunapala, J. K. Liu, S. V. Bandara, W. Hong, P. D. Maker, R. E. Muller and T. N. Krabach

ABSTRACT

In this paper, we discuss the development of very sensitive long wavelength infrared $GaAs/Al_xGa_{1-x}As$ quantum well infrared photodetectors (QWIPs) based on bound-to-quasibound intersubband transition, fabrication of ligh coupling schemes for efficient light coupling, and demonstration of several long wavelength infrared cameras based on QWIP focal plane arrays. Excellent imagery, with a noise equivalent differential temperature (NEΔT) of 30 mK have been achieved in demonstrations.

INTRODUCTION

There are many applications that require long wavelength, large, uniform, reproducible, low cost, low 1/f noise, low power dissipation, and radiation hard infrared (IR) focal plane arrays (FPAs). For example, the absorption lines of many gas molecules, such as ozone, water, carbon monoxide, carbon dioxide, and nitrous oxide occur in the wavelength region from 3 to 18 µm. Thus, IR imaging systems that operate in the long wavelength IR (LWIR) region (8 - 18 µm) are required in many space applications such as monitoring the global atmospheric temperature profiles, relative humidity profiles, cloud characteristics, and the distribution of minor constituents in the atmosphere which are being planned for NASA's Earth Observing System [1]. In addition, 8-15 µm FPAs would be very useful in detecting cold objects such as ballistic missiles in midcourse (when hot rocket engine is not burning most of the emission peaks are in the 8-15 µm IR region) [2]. The GaAs based Quantum Well Infrared Photodetector (QWIP) [3] is a potential candidate for such space borne applications and it can meet all of the requirements mentioned above for this spectral region.

A quantum well designed to detect infrared (IR) light is called a quantum well infrared photodetector (QWIP). An elegant candidate for QWIP is the square quantum well of basic quantum mechanics [3]. When the quantum well is sufficiently deep and narrow, its energy states are quantized (discrete). The potential depth and width of the well can be adjusted so that it holds only two energy states: a ground state near the well bottom, and a first excited state near the well top. A photon striking the well will excite an electron in the ground state to the first excited state, then an externally-applied voltage sweeps it out producing a photocurrent. Only photons having energies corresponding to the energy separation between the two states are absorbed, resulting in a detector with a sharp absorption spectrum. Designing a quantum well to detect light of a particular wavelength becomes a simple matter of tailoring the potential depth and width of the well to produce two states separated by the desired photon energy. The $GaAs/Al_xGa_{1-x}As$ material system allows the quantum well shape to be tweaked over a range wide enough to enable light detection at wavelengths longer than ~ 6 µm. Fabricated entirely from large bandgap materials which are easy to grow and process, it is now possible to obtain large uniform FPAs of QWIPs tuned to detect light at wavelengths from 6 to 25 µm in the $GaAs/Al_xGa_{1-x}As$ material system [3].

Improving QWIP performance depends largely on minimizing the parasitic current that plagues all light detectors, the dark current (the current that flows through a biased detector in the dark, i.e., with no photons impinging on it). As we have discussed elsewhere [3], at temperatures above 45 K, the dark current of the QWIP is entirely dominated by classic thermionic emission of ground state electrons directly out of the well into the energy continuum. Minimizing this last component is critical to the commercial success of the QWIP as it allows the highly-desirable high-temperature camera operation. Therefore, we have designed the *bound-to-quasibound* quantum well by placing the first excited state exactly at the well top as shown in Fig. 1. The best previous QWIPs (pioneered by Barry Levine *et al.* at AT&T Bell Labs) were of the bound-to-continuum variety, so-called because the first excited state was a continuum energy band above the well top (typically 10 meV). Dropping the first excited state to the well top causes the barrier to thermionic emission (roughly the energy height from the ground state to the well top) to be ~ 10 meV more in our bound-to-quasibound QWIP than in the bound-to-continuum one, theoretically causing the dark current to drop by a factor of ~ 6 at a temperature of 70 K [3].
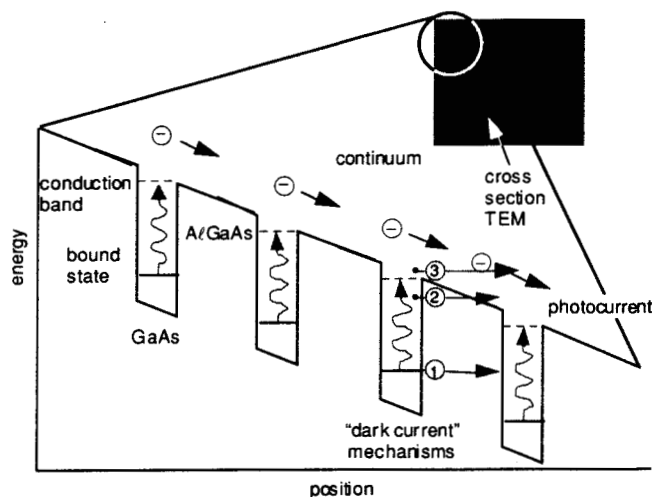

Figure 1. Schematic diagram of the conduction band in a bound-to-quasi-bound QWIP in an externally applied electric field. Absorption of IR photons can photoexcite electrons from the ground state of the quantum well into the continuum, causing a photocurrent. Three dark current mechanisms are also shown: 1) ground-state tunneling; 2) thermally-assisted tunneling; and 3) thermionic emission. The inset shows a cross section transmission electron micrograph of a QWIP sample.

TEST STRUCTURE RESULTS (14-15 MICRONS)

The device structure consists of 50 periods containing 65 Å wells of GaAs (doped $n = 2x10^{17}$ cm^{-3}) and 600 Å barriers of $Al_{0.15}Ga_{0.85}As$ (sandwiched between 0.5 µm GaAs top and bottom contact layers doped $n = 2x10^{17}$ cm^{-3}) grown on a semi-insulating GaAs substrate by molecular beam epitaxy (MBE). Then a 1.1 µm thick GaAs cap layer on top of 300 Å

$Al_{0.15}Ga_{0.85}As$ stop-etch layer was grown *in situ* on top of the device structure to fabricate the light coupling optical cavity. The MBE grown QWIP structure was processed into 200 μm diameter mesa test structures (area = 3.14 x 10^{-4} cm^2) using wet chemical etching, and Au/Ge ohmic contacts were evaporated onto the top and bottom contact layers. The responsivity spectra of these detectors were measured using a 1000 K blackbody source and a grating monochromator. The absolute peak responsivities (R_p) of the detectors were measured using a calibrated blackbody source. The detector were back illuminated through a 45° polished facet [3] and its responsivity spectrum is shown in Fig. 2. The responsivity of the detector peak at 14.2 μm and the peak responsivity (R_p) of the detector is 420 mA/W. The spectral width and the cutoff wavelength are $\Delta\lambda / \lambda$ = 13% and λ_C = 14.9 μm.

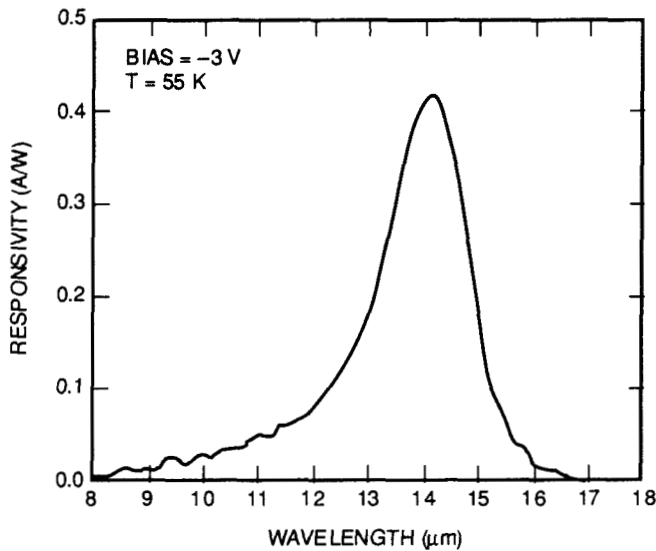*Figure 2. Responsivity spectra of a bound-to-quasi-continuum VWIR QWIP focal plane array sample at temperature T = 55 K. The spectral response peak at 14.2 μm and the long wavelength cutoff is at 14.9 μm.*

TEST STRUCTURE RESULTS (8-9 MICRONS)

Each period of the multi-quantum well (MQW) structure consists of a 45 Å well of GaAs (doped n = 4×10^{17} cm^{-3}) and a 500 Å barrier of $Al_{0.3}Ga_{0.7}As$. Stacking many identical quantum wells (typically 50) together increases photon absorption. Ground state electrons are provided in the detector by doping the GaAs well layers with Si. This photosensitive MQW structure is sandwiched between 0.5 μm GaAs top and bottom contact layers doped n = 5×10^{17} cm^{-3}, grown on a semi-insulating GaAs substrate by molecular beam epitaxy (MBE). Then a 0.7 μm thick GaAs cap layer on top of a 300 Å $Al_{0.3}Ga_{0.7}As$ stop-etch layer was grown *in situ* on top of the device structure to fabricate the light coupling optical cavity.

The detectors were back illuminated through a 45° polished facet as described earlier and a responsivity spectrum is shown in Fig. 3. The responsivity of the detector peaks at 8.5 μm and the peak responsivity (R_p) of the detector is 300 mA/W at bias V_B = -3 V. The spectral width and the cutoff wavelength are $\Delta\lambda / \lambda$ = 10% and λ_C = 8.9 μm respectively. The bias dependent peak responsivity of the detector is shown in Fig. 4.
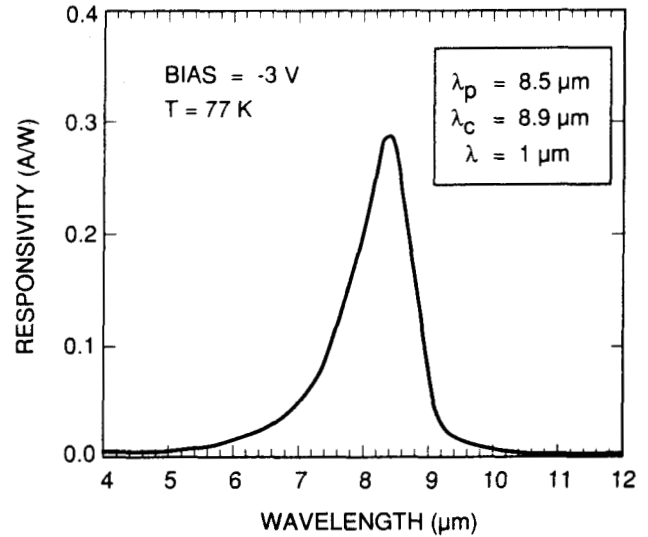

Figure 3. Responsivity spectrum of a bound-to-quasi-bound LWIR QWIP test structure at temperature T = 77 K. The spectral response peak is at 8.5 μm and the long-wavelength cutoff is at 8.9 μm.
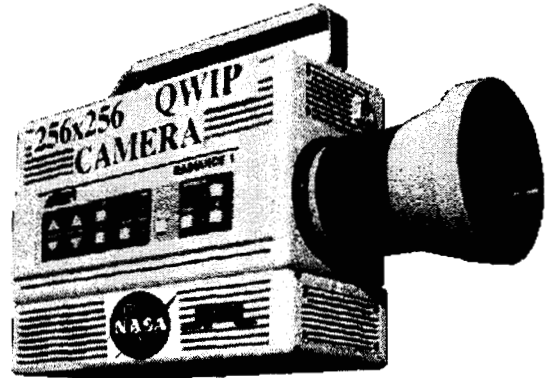

Figure 4. Picture of the first 256 x 256 hand-held long wavelength QWIP camera (QWIP RADIANCE).

The measured absolute peak responsivity of the detector is small, up to about V_B = -0.5 V. Beyond that it increases nearly linearly with bias reaching R_p = 380 mA/W at V_B = -5 V. This type of behavior of responsivity versus bias is typical for a bound-to-quasibound QWIP. The peak quantum efficiency was 6.9% at bias V_B = -1 V for a 45° double pass. The lower quantum efficiency is due to the lower well doping density (5×10^{17} cm^{-3}) as it is necessary to suppress the dark current at the highest possible operating temperature.

14-15 MICRON 128X128 QWIP IMAGING CAMERA

It is well known that QWIPs do not absorb radiation incident normal to the surface unless the IR radiation have an electric field component normal to the layers of superlattic e (growth direction) [3]. As we have discussed before [3] many more passes of IR light inside the detector structure can be obtained by incorporating a randomly roughened reflecting surface on top of the detectors which also removes the light coupling limitations and makes two dimensional QWIP imaging arrays feasible. The photoconductive QWIPs of the 128x128 FPAs were then fabricated by wet chemical etching through the

photosensitive GaAs/Al$_x$Ga$_{1-x}$As multi quantum well layers into the 0.5 μm thick doped GaAs contact layer. The pitch of the FPA is 50 μm and the actual pixel size is 38x38 μm^2. Then the random reflectors on the top of the detectors were covered with Au/Ge and Au for Ohmic contact and reflection. Then indium bumps were evaporated on top of the detectors for Si read out circuit (ROC) hybridization. A single QWIP FPA was chosen (cutoff wavelength of this sample is 14.9 μm) and bonded to a 128x128 Si multiplexer (Amber AE-159) and biased at V_b = -2.7 V. The FPA was back-illuminated through the flat thinned substrate (thickness ≈ 25 μm). This initial array gave excellent images with 99.9% of the pixels working, demonstrating the high yield of GaAs technology. Excellent uncorrected photocurrent uniformity (pixel-to-pixel) of the 16384 pixels of the 128x128 FPA is achieved with a standard deviation of only σ =2.4%. [4] The residual non-uniformity after correction was 0.05% and it is excellent compared to other types of focal plane arrays in the same wavelength region.

8-9 MINCRON 256X256 QWIP HAND-HELD CAMERA

After the random reflector array was defined by the lithography and dry etching, the photoconductive QWIPs of the 256x256 FPAs were fabricated by wet chemical etching through the photosensitive GaAs/Al$_x$Ga$_{1-x}$As multi-quantum well layers into the 0.5 μm thick doped GaAs bottom contact layer. The pitch of the FPA is 38 μm and the actual pixel size is 28x28 μm^2. The random reflectors on top of the detectors were then covered with Au/Ge and Au for Ohmic contact and reflection. A single QWIP FPA was chosen and hybridized (via indium bump-bonding process) to a 256x256 CMOS multiplexer (Amber AE-166) and biased at V_B = -1.0 V. The FPA was back-illuminated through the flat thinned substrate membrane (thickness ≈ 1300 Å). This initial array gave excellent images with 99.98% of the pixels working (number of dead pixels ≈ 10) , demonstrating the high yield of GaAs technology. The measured NEΔT of the FPA at an operating temperature of T = 70 K, bias V_B = -1 V for 300 K background and the mean value is 26 mK. This agrees reasonably with our estimated value of 8 mK based on test structure data. The peak quantum efficiency of the FPA was 3.3% (lower focal plane array quantum efficiency is attributed to 54% fill factor and 90% charge injection efficiency) and this corresponds to an average of three passes of IR radiation (equivalent to a single 45° pass) through the photosensitive multi-quantum well region.

A 256x256 QWIP FPA hybrid was mounted onto a 250 mW integral Sterling closed-cycle cooler assembly and installed into an Amber RADIANCE 1^{TM} camera-body, to demonstrate a hand-held LWIR camera (shown in Fig. 4). The camera is equipped with a 32-bit floating-point digital signal processor combined with multi-tasking software, providing the speed and power to execute complex image-processing and analysis functions inside the camera body itself. The other element of the camera is a 100 mm focal length germanium lens, with a 5.5 degree field of view. It is designed to be transparent in the 8-12 μm wavelength range, to be compatible with the QWIP's 8.5 μm operation. The digital acquisition resolution of the camera is 12-bits, which determines the instantaneous dynamic range of the camera (i.e., 4096). However, the dynamic range of QWIP is 85 Decibels. Its nominal power consumption is less than 50 Watts [5].

8-9 MICRON 640X486 QWIP IMAGING CAMERA

Although random reflectors have achieved relatively high quantum efficiencies with large test device structures, it is not possible to achieve the similar high quantum efficiencies with random reflectors on small focal plane array pixels due to the reduced width-to-height aspect ratios. In addition, it is difficult to fabricate random reflectors for shorter wavelength detectors relative to very long-wavelength detectors (i.e., 15 μm) due to the fact that feature sizes of random reflectors are linearly proportional to the peak wavelength of QWIPs. As we have discussed before (3), more IR light can be coupled to the QWIP detector structure by incorporating a two dimensional grating surface on top of the detectors which also removes the light coupling limitations and makes two dimensional QWIP imaging arrays feasible.

After the 2-D grating array was defined by the photolithography and dry etching, the photoconductive QWIPs of the 640x486 FPAs were fabricated by wet chemical etching through the photosensitive GaAs/Al$_x$Ga$_{1-x}$As multi-quantum well layers into the 0.5 μm thick doped GaAs bottom contact layer. The pitch of the FPA is 25 μm and the actual pixel size is 18x18 μm^2. The cross gratings on top of the detectors were then covered with Au/Ge and Au for Ohmic contact and reflection. A single QWIP FPA was chosen and hybridized to a 640x486 direct injection silicon readout multiplexer (Amber AE-181) and biased at V_B = -2.0 V. The FPA was back-illuminated through the flat thinned substrate membrane (thickness ≈ 1300 Å). This thinned GaAs FPA membrane has completely eliminated the thermal mismatch between the silicon CMOS readout multiplexer and the GaAs based QWIP FPA. Basically, the thinned GaAs based QWIP FPA membrane adapts to the thermal expansion and contraction coefficients of the silicon readout multiplexer. Therefore, this thinning has played an extremely important role in the fabrication of large area FPA hybrids. In addition, this thinning has completely eliminated the pixel-to-pixel optical cross-talk of the FPA. This initial array gave excellent images with 99.9% of the pixels working, demonstrating the high yield of GaAs technology. Figure 5 shows the experimentally measured NEΔT of the FPA at an operating temperature of T = 70 K, bias V_B = -2 V at 300 K background and the mean value 36 mK. This agrees reasonably with our estimated value of 25 mK based on test structure data. The experimentally measured peak quantum efficiency of the FPA was 2.3% (lower focal plane array quantum efficiency is attributed to 51% fill factor and 30% reflection loss from the GaAs back surface). Therefore, the corrected quantum efficiency of a focal plane detectors is 6.5% and this corresponds to an average of two pass of IR radiation (equivalent to a single 45° pass) through the photosensitive multi-quantum well region.

A 640X486 QWIP FPA hybrid was mounted onto a 84-pin lead-less chip carrier and installed into a laboratory dewar which is cooled by liquid nitrogen to demonstrate a LWIR imaging camera). The other element of the camera is a 100 mm focal length AR coated germanium lens, which gives a 9.2°x6.9° field of view. The measured mean NEΔT of the QWIP camera is 36 mK at an operating temperature of T = 70 K and bias V_B = -2 V at 300 K background. The uncorrected NEΔT non-uniformity of the 640x486 FPA is about 5.6% (= sigma/ mean).

Video images were taken at a frame rate of 30 Hz at temperatures as high as T = 70 K using a ROC capacitor having a charge

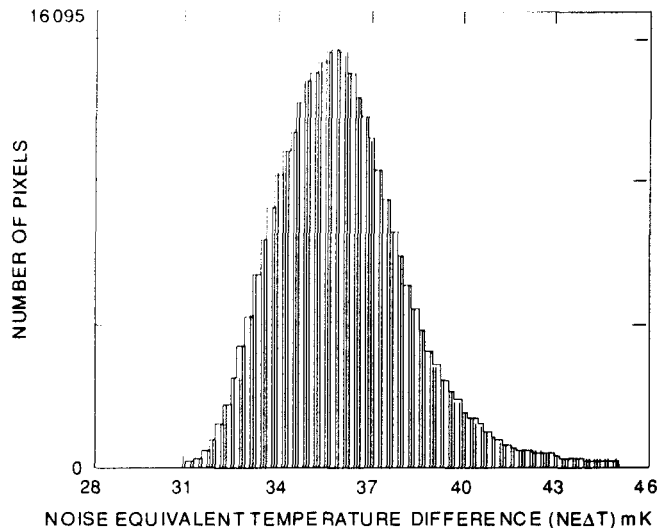*Figure 5. Noise equivalent temperature difference (NEΔT) histogram of the 311,040 pixels of the 640 x 486 array showing a high uniformity of the FPA. The uncorrected non-uniformity (= standard deviation/mean) of this unoptimized FPA is only 5.6% including 1% non-uniformity of ROC and 1.4% non-uniformity due to the cold-stop not being able to give the same field of view to all the pixels in the FPA.*

capacity of 9×10^6 electrons. The non-uniformity after two-point ($17°$ and $27°$ Celsius) correction improves to an impressive 0.1%. Figure 6 shows a frame of video image taken with this long-wavelength 640x486 QWIP camera. This image demonstrates the high sensitivity of the 640 x 486 long-wavelength QWIP staring array camera. As mentioned earlier, this high yield is due to the excellent GaAs growth uniformity and the mature GaAs processing technology.

Figure 6. This picture was taken in the night (around midnight) and it clearly shows where automobiles were parked during the day time. This image demonstrates the high sensitivity of the 640 x 486 long-wavelength QWIP staring array camera.

REFERENCES

[1] M. T. Chahine, "Sensor requirements for Earth and Planetary Observations," *Proceedings of Innovative Long Wavelength Infrared Detector Workshop*, Pasadena, California, pp. 3-31, April 24-26, 1990.

[2] D. Duston, "BMDO's IS&T faces new hi-tech priorities", *BMD Monitor*, pp 180-183, May 19, 1995.

[3] S. D. Gunapala and K. M. S. V. Bandara, Physics of Thin Films, Academic Press, **21**, 113 (1995).

[4] S. D. Gunapala, J. S. Park, G. Sarusi, T. L. Lin, J. K. Liu, P. D. Maker, R. E. Muller, C. A. Shott, T. Hoelter, and B. F. Levine "128 x 128 GaAs/Al_xGa_{1-x}As Quantum Well Infrared Photodetector Focal Plane Array for Imaging at 15 μm," IEEE Trans. Electron Devices, **44**, pp. 45-50, 1997.

[5]. Sarath D. Gunapala, John K. Liu, Jin S. Park, Mani Sundaram, Craig A. Shott, Ted Hoelter, True-Lon Lin, S. T. Massie, Paul D. Maker, Richard E. Muller, and Gabby Sarusi" 9 μm Cutoff 256x256 GaAs/Al_xGa_{1-x}As Quantum Well Infrared Photodetector Hand-Held Camera", IEEE Trans. Electron Devices, **44**, pp. 51-57, 1997.